

Figure 2. Relative quantitation of phosphopeptides between two groups from breast tissues by SRM. The scatter plots indicate the peak area ratio of the internal peptide to SI peptide and each horizontal bar indicates the mean value. Y-axis shows the normalized peak area. The “internal peptide” and “SI peptide” are based on the transition from internal peptides and SI peptides, respectively. (A) indicates significant difference groups ($p < 0.05$), (B) different propensity ($p > 0.05, < 0.2$), and (C) no significant difference between two groups ($p > 0.2$). Closed circle indicates samples that were satisfactorily quantified.

Table 4. SRM-Based Quantification of Phosphopeptides^a

gene symbol	Uniprot accession	protein name	targeted phosphopeptide	phosphorylated site	high/low ratio	T. TEST	area ratio (unlabeled/stable-isotope labeled peptide)																
							H01	H04	H06	H07	H08	H09	L11	L13	L14	L15	L16	L17					
RPL23A	P62750	60S ribosomal protein L23a	IRTpSPTFR	S43	0.20	0.149	3.8×10^{-1}	2.8×10^{-1}	2.4×10^{-1}	2.3×10^{-1}	1.4×10^{-1}	9.5×10^{-2}	1.0×10^{-1}	6.5×10^{-2}	3.2×10^{-2}	3.1×10^{-1}	1.4×10^{-1}	ND					
MX1	P20591	Interferon-induced GTP-binding protein Mx1	WpSEVDIAK	S4	3.94	0.123	2.1×10^{-2}	6.0×10^{-2}	2.9×10^{-2}	1.4×10^{-1}	3.2×10^{-2}	ND	1.1×10^{-2}	1.5×10^{-2}	ND	ND	2.0×10^{-2}	1.0×10^{-2}					
CDK1 CDK2 CDK3	P06493 P24941 Q00526	Cell division protein kinase 1/2/3	IGEGpTYGWYK	T14	6.99	0.077	1.9×10^{-2}	4.8×10^{-2}	1.7×10^{-2}	8.9×10^{-2}	7.2×10^{-3}	1.6×10^{-2}	5.1×10^{-3}	ND	5.4×10^{-3}	7.5×10^{-3}	2.8×10^{-3}	2.4×10^{-3}					
LMO7	Q8WW11	LIM domain only protein 7	pSYTSDLOK	S417	3.07	0.048	2.2×10^{-2}	5.0×10^{-2}	1.4×10^{-2}	3.5×10^{-2}	8.5×10^{-2}	3.2×10^{-2}	1.3×10^{-2}	ND	6.4×10^{-3}	9.0×10^{-3}	2.0×10^{-2}	1.7×10^{-2}					
ALGS	Q92685	Dolichyl-P-Man ₇ Man(5)GlcNAc(2)-PP-dolichyl mannosyltransferase	SGpSAAQAEGGLCK	S13	2.74	0.049	2.1×10^{-1}	2.1×10^{-1}	1.4×10^{-1}	2.1×10^{-1}	5.1×10^{-2}	2.6×10^{-2}	4.5×10^{-2}	2.8×10^{-2}	5.1×10^{-3}	6.0×10^{-2}	1.7×10^{-2}	8.7×10^{-2}					
PDSSA	Q29RF7-1	Sister chromatid cohesion protein PDSS homologue A	IISVpTPVK	T1208	5.14	0.044	6.7×10^{-2}	2.3×10^{-1}	2.1×10^{-2}	2.6×10^{-1}	1.0×10^{-1}	3.6×10^{-2}	2.4×10^{-2}	1.1×10^{-2}	1.7×10^{-2}	3.1×10^{-2}	1.9×10^{-2}	3.7×10^{-2}					
CCR1	P32246	C-C chemokine receptor type 1	VSSTSPSTGEHELpSAGF	S352	2.34	0.046	1.3×10^{-1}	1.4×10^{-1}	9.0×10^{-2}	1.0×10^{-1}	3.8×10^{-2}	2.7×10^{-2}	3.4×10^{-2}	ND	3.1×10^{-2}	2.5×10^{-2}	4.2×10^{-2}	5.7×10^{-2}					
MCM2	O95297-1	DNA replication licensing factor MCM2	GLLYDpSDEEDEERPAR	S139	5.30	0.156	3.6×10^{-1}	2.0	2.5×10^{-1}	2.1	3.9×10^{-2}	1.3×10^{-1}	1.3×10^{-1}	ND	9.4×10^{-2}	2.8×10^{-1}	3.3×10^{-2}	2.3×10^{-1}					
CDK1 CDK2 CDK3	P60493 P24941 Q00526	Cell division protein kinase 1/2/3	IGEGTpYGWYK	Y15	5.09	0.074	1.0×10^{-1}	1.1×10^{-1}	1.5×10^{-2}	2.1×10^{-1}	2.5×10^{-2}	4.0×10^{-2}	1.5×10^{-2}	ND	6.3×10^{-3}	1.8×10^{-2}	2.1×10^{-2}	2.0×10^{-2}					
MPZL1	O95297-1	Myelin protein zero-like protein 1	SESVVpYADIR	Y263	0.39	0.183	1.2×10^{-1}	2.1×10^{-1}	1.7×10^{-1}	1.5×10^{-1}	9.7×10^{-2}	1.7×10^{-1}	4.6×10^{-1}	1.5×10^{-1}	3.8×10^{-1}	1.1	1.3×10^{-1}	1.3×10^{-1}					
KRT8	P05787	Keratin, type II cytoskeletal 8	YEELQpSLAGK	S291	0.81	0.533	ND	3.5×10^{-2}	1.8×10^{-2}	5.4×10^{-2}	2.6×10^{-2}	1.9×10^{-2}	3.9×10^{-2}	ND	6.6×10^{-2}	4.9×10^{-2}	2.7×10^{-2}	1.2×10^{-2}					
MUC1	P15941-1	Mucin-1	YVPPSSSTRpSPYK	S1227	3.10	0.170	0.63	0.46	0.72			0.64	1.02	1.1	2.03		1.84	1.28					
PKP2	Q99959-1	Plakophilin-2	LELpSPDSSPER	S151	0.37	0.243	0.07	0.27	0.16	0.48	0.34	0.3	1.11	0.32	0.22	5.96	0.84	0.78					
INADL	Q8NI35-1	InaD like protein	LFDDApSVDEPR	S645	1.08	0.834	1.1×10^{-2}	9.3×10^{-3}	4.0×10^{-3}	1.1×10^{-2}	ND	ND	1.5×10^{-2}	4.8×10^{-3}	3.9×10^{-3}	1.5×10^{-2}	2.9×10^{-3}	8.5×10^{-3}					
SHROOM3	Q8TF72-1	shroom family member 3 protein	pSPLNSPPVKPK	S439	0.46	0.071	6.9×10^{-3}	4.7×10^{-3}	1.9×10^{-3}	3.7×10^{-3}	1.9×10^{-3}	6.3×10^{-3}	1.0×10^{-3}	2.8×10^{-3}	4.3×10^{-3}	1.3×10^{-3}	ND	1.5×10^{-3}					

^aND: not detected.

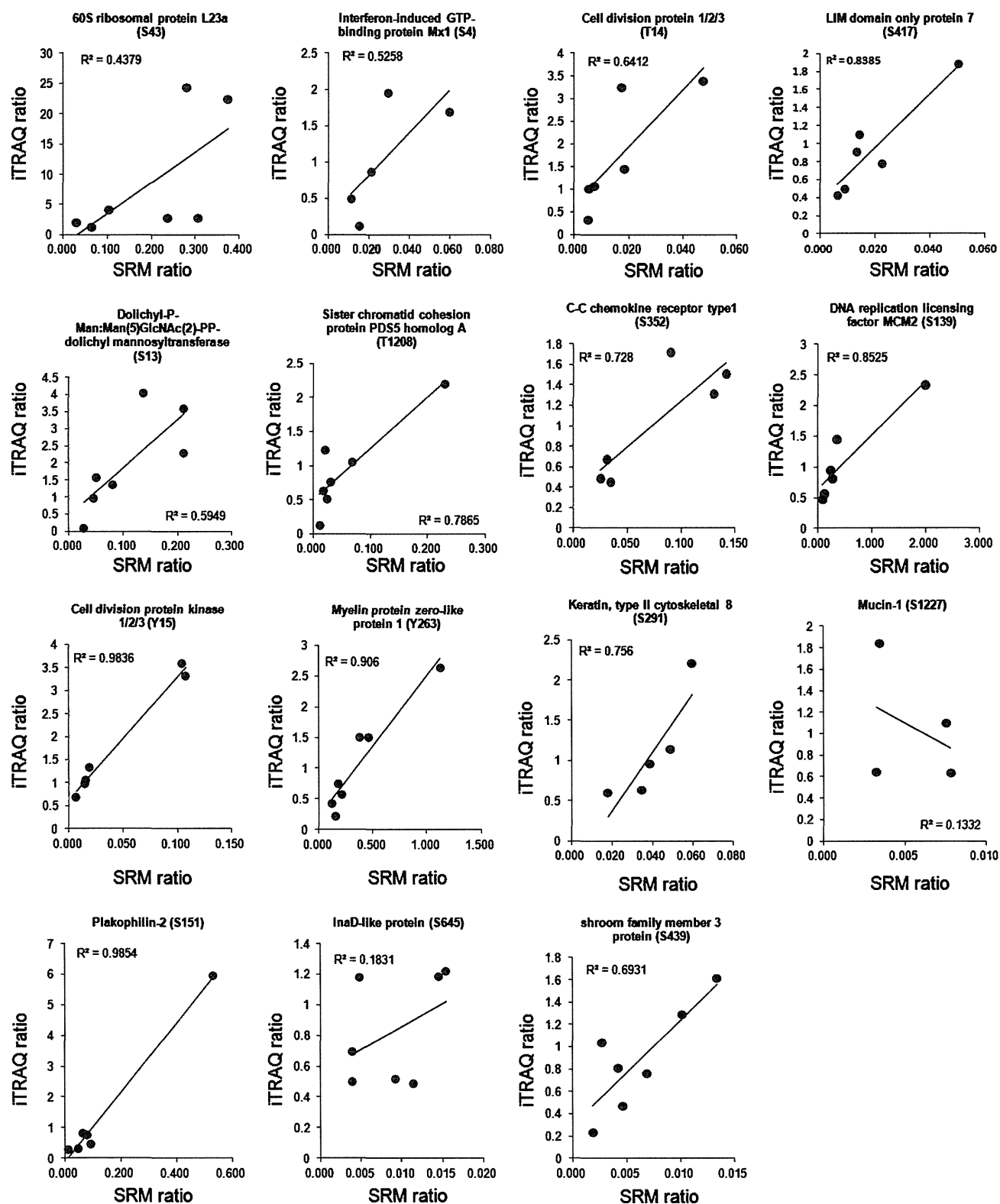


Figure 3. Linear regression comparing peptide ratio results obtained by iTRAQ and SRM assay. The iTRAQ and SRM ratios were plotted on each graph. Each data point represents a given peptide ratio in the same samples, which were quantified by either iTRAQ or SRM assay. Correlation coefficients are shown in plots.

phosphorylation site. For example, FVpSEGDGGR (fold change: 0.26) and RFVpSEGDGGR (0.48) peptides with pS457 of programmed cell death protein 4 and AGGSAALpSPSK (2.49) and AGGSAALpSPSKK (2.08) peptides with pS31 of Histone H1x both showed significant

differences between high- and low-risk groups (Supporting Information Table S4), which would indicate that our large-scale phosphoproteomic analysis had sufficient quantitative reproducibility to search for putative phosphoprotein biomarkers.

Verification of the phosphorylation state is essential in the search for phospho-biomarkers. If specific and well-characterized antibodies for these candidates are available, the validation step could be performed easily using Western blotting and ELISA. However, highly specific antibodies for most phosphoproteins are not available, and the development of good antibodies that recognize a specific phosphorylation frame is a cumbersome, expensive and time-consuming process that requires a priori knowledge of the protein and its phosphorylation sites. On the other hand, SRM does not require antibodies and is able to validate multiple phosphorylation sites within a single run. Recently, SRM analysis was used to validate the evidence for a large-scale proteome;^{55–57} however, phosphopeptide SRM has only been performed for specific protein phosphorylation such as Akt,⁵⁸ Lyn,⁵⁹ EGFR⁶⁰ or tyrosine phosphorylated peptides after EGF treatment.⁶¹ In this study, we selected and validated 19 phosphopeptides from 133 biomarker candidate phosphopeptides of breast cancer tissue discovered by iTRAQ-based phosphoproteomics. To our knowledge, this study is the first to validate phosphopeptides discovered by large-scale phosphoproteomic analysis using SRM.

Recently, several reports identified biomarker candidates by quantitative shotgun proteomics and subsequent validation by SRM,^{57,62} but these studies carried out the SRM assay without SI peptides. Although this method has the advantage of reducing the cost and time for SI peptide synthesis, difficulties occur in SRM analysis without internal standards, which provide the correct retention time for target peptides and verify the specificity of the analyte.⁵⁶ Also, the use of SI peptide provides the most favorable SRM information, such as the highest intensity fragment ions for each peptide. Thus, inclusion of SI peptides as an internal control is indispensable, especially for quantitation of low-abundance proteins such as phosphopeptide. Whiteaker et al. pointed out that the choice of candidates for quantitative SRM assay development was limited to the most abundant proteins or peptides without internal standards.⁵⁶ Our successful quantitation of low abundant phosphopeptides was largely a result of the inclusion of SI peptides.

In this study, only four of 15 potential biomarker candidate phosphopeptides quantified by iTRAQ showed a significant difference between high- and low-risk groups of breast cancer (Figure 2) and quantification of the amount of phosphopeptides by iTRAQ and SRM was not always correlated (Figure 3). Several reasons could be considered for the discrepancy. First, the sample size used for both discovery and verification was very small. In addition to the four phosphopeptides with a significant difference obtained by our SRM analysis, eight candidate phosphopeptides showed quite different expressions, although not significantly, between high- and low-risk groups. If we could increase the number of samples, more biomarker candidate phosphopeptides identified by the discovery approach could be verified. Second, quantitative variation might be generated in the discovery phase of phosphoproteomics. This includes one additional step of phosphopeptide enrichment by IMAC as compared with the usual iTRAQ method, which might create such variation. Moreover, the heterogeneity of cancer tissue samples could further highlight quantitative variation in a step of phosphopeptide enrichment. This is evidenced by the fact that good reproducibility and correlation were obtained between the quantitation of phosphopeptides by iTRAQ and SRM when their analysis was performed using samples prepared from cell lysate (data not shown). Phosphopeptide enrichment might be more sensitive to the composition of the

sample and the solution used for lysis or digestion of protein extracts; therefore, validation by SRM analysis is very important for the biomarker candidate phosphopeptides discovered by iTRAQ analysis combined with IMAC. Third, the endogenous phosphopeptide level is near the limit of quantitation so that the number of phosphopeptides quantified even with highly sensitive SRM was not accurate enough. We have observed that iTRAQ-based discovery and SRM-based validation of biomarker candidates of membrane proteins obtained from breast cancer tissues were well correlated.⁶³ This was probably due to the abundance of membrane proteins as compared with phosphoprotein. Thus, further improvement of the sensitivity of SRM is needed for accurate quantitation of low-abundance protein such as phosphoprotein.

In conclusion, we performed a large-scale phosphoproteome quantification and subsequent SRM-based validation using breast cancer tissue samples. The significance of this study is to provide a strategy for the quantitation and validation of low-abundance phosphopeptides using the most recent proteomic technologies, which might lead to a fundamental shift from traditional validation using antibodies. Quantitation of phosphopeptides by SRM will be applied to examine various kinase activities and signaling pathways in cells in the near future.

■ ASSOCIATED CONTENT

📄 Supporting Information

Figure S1. Schematic workflow of iTRAQ analysis combined with IMAC for identification of potential biomarkers and SRM analysis combined with IMAC for validation. Figure S2. Venn diagram of the phosphopeptides identified in the four experiments of iTRAQ-based proteomic analysis. Figure S3. Expression of Mucin-1 protein in breast cancer tissues. Table S1. Patient information in experiment. Table S2. Identified phosphopeptides. Table S3. Quantified phosphopeptides. Table S4. Phosphopeptides with significant difference between two groups by iTRAQ analysis. Table S5. Transition list of target phosphopeptides. This material is available free of charge via the Internet at <http://pubs.acs.org>.

■ AUTHOR INFORMATION

Corresponding Author

*Tel: +81-72-641-9862. Fax: +81-72-641-9861. E-mail: tomonaga@nibio.go.jp.

Author Contributions

#Ryohei Narumi and Tatsuo Murakami contributed equally to this paper.

Notes

The authors declare no competing financial interest.

■ ACKNOWLEDGMENTS

This work was supported by a Grant-in-Aid for Research on Biological Markers for New Drug Development H20-0005 to T.T. from the Ministry of Health, Labour and Welfare of Japan and by Grant-in-Aid 21390354 to T.T. from the Ministry of Education, Science, Sports and Culture of Japan.

■ ABBREVIATIONS

iTRAQ, isobaric peptide tags for relative and absolute quantification; SRM, selected reaction monitoring; IMAC, immobilized metal affinity chromatography; SI peptide, stable isotope-labeled peptide; SCX, strong cation exchange; CID,

collision-induced dissociation; HCD, higher energy collision-induced dissociation; LC-MS/MS, liquid chromatography-tandem mass spectrometry; CE, collision energy; LTQ, linear ion trap; fwhm, full width at half-maximum; FDR, false discovery rate

REFERENCES

- (1) Hanahan, D.; Weinberg, R. A. The hallmarks of cancer. *Cell* **2000**, *100* (1), 57–70.
- (2) Kaminska, B. MAPK signalling pathways as molecular targets for anti-inflammatory therapy—from molecular mechanisms to therapeutic benefits. *Biochim. Biophys. Acta* **2005**, *1754* (1–2), 253–62.
- (3) Peifer, C.; Wagner, G.; Laufer, S. New approaches to the treatment of inflammatory disorders small molecule inhibitors of p38 MAP kinase. *Curr. Top. Med. Chem.* **2006**, *6* (2), 113–49.
- (4) White, M. F. Regulating insulin signaling and beta-cell function through IRS proteins. *Can. J. Physiol. Pharmacol.* **2006**, *84* (7), 725–37.
- (5) Neville, D. C.; Rozanas, C. R.; Price, E. M.; Gruis, D. B.; Verkman, A. S.; Townsend, R. R. Evidence for phosphorylation of serine 753 in CFTR using a novel metal-ion affinity resin and matrix-assisted laser desorption mass spectrometry. *Protein Sci.* **1997**, *6* (11), 2436–45.
- (6) Ong, S. E.; Blagoev, B.; Kratchmarova, I.; Kristensen, D. B.; Steen, H.; Pandey, A.; Mann, M. Stable isotope labeling by amino acids in cell culture, SILAC, as a simple and accurate approach to expression proteomics. *Mol. Cell. Proteomics* **2002**, *1* (5), 376–86.
- (7) Ross, P. L.; Huang, Y. N.; Marchese, J. N.; Williamson, B.; Parker, K.; Hattan, S.; Khainovski, N.; Pillai, S.; Dey, S.; Daniels, S.; Purkayastha, S.; Juhasz, P.; Martin, S.; Bartlett-Jones, M.; He, F.; Jacobson, A.; Pappin, D. J. Multiplexed protein quantitation in *Saccharomyces cerevisiae* using amine-reactive isobaric tagging reagents. *Mol. Cell. Proteomics* **2004**, *3* (12), 1154–69.
- (8) Collins, M. O.; Yu, L.; Coba, M. P.; Husi, H.; Campuzano, I.; Blackstock, W. P.; Choudhary, J. S.; Grant, S. G. Proteomic analysis of in vivo phosphorylated synaptic proteins. *J. Biol. Chem.* **2005**, *280* (7), 5972–82.
- (9) Molina, H.; Horn, D. M.; Tang, N.; Mathivanan, S.; Pandey, A. Global proteomic profiling of phosphopeptides using electron transfer dissociation tandem mass spectrometry. *Proc. Natl. Acad. Sci. U. S. A.* **2007**, *104* (7), 2199–204.
- (10) Wissing, J.; Jansch, L.; Nimitz, M.; Dieterich, G.; Hornberger, R.; Keri, G.; Wehland, J.; Daub, H. Proteomics analysis of protein kinases by target class-selective prefractionation and tandem mass spectrometry. *Mol. Cell. Proteomics* **2007**, *6* (3), 537–47.
- (11) Villen, J.; Beausoleil, S. A.; Gerber, S. A.; Gygi, S. P. Large-scale phosphorylation analysis of mouse liver. *Proc. Natl. Acad. Sci. U. S. A.* **2007**, *104* (5), 1488–93.
- (12) Ballif, B. A.; Villen, J.; Beausoleil, S. A.; Schwartz, D.; Gygi, S. P. Phosphoproteomic analysis of the developing mouse brain. *Mol. Cell. Proteomics* **2004**, *3* (11), 1093–101.
- (13) Beausoleil, S. A.; Jedrychowski, M.; Schwartz, D.; Elias, J. E.; Villen, J.; Li, J.; Cohn, M. A.; Cantley, L. C.; Gygi, S. P. Large-scale characterization of HeLa cell nuclear phosphoproteins. *Proc. Natl. Acad. Sci. U. S. A.* **2004**, *101* (33), 12130–5.
- (14) Ficarro, S. B.; McClelland, M. L.; Stukenberg, P. T.; Burke, D. J.; Ross, M. M.; Shabanowitz, J.; Hunt, D. F.; White, F. M. Phosphoproteome analysis by mass spectrometry and its application to *Saccharomyces cerevisiae*. *Nat. Biotechnol.* **2002**, *20* (3), 301–5.
- (15) Lee, J.; Xu, Y.; Chen, Y.; Sprung, R.; Kim, S. C.; Xie, S.; Zhao, Y. Mitochondrial phosphoproteome revealed by an improved IMAC method and MS/MS. *Mol. Cell. Proteomics* **2007**, *6* (4), 669–76.
- (16) Moser, K.; White, F. M. Phosphoproteomic analysis of rat liver by high capacity IMAC and LC-MS/MS. *J. Proteome Res.* **2006**, *5* (1), 98–104.
- (17) Trinidad, J. C.; Specht, C. G.; Thalhammer, A.; Schoepfer, R.; Burlingame, A. L. Comprehensive identification of phosphorylation sites in postsynaptic density preparations. *Mol. Cell. Proteomics* **2006**, *5* (5), 914–22.
- (18) Li, X.; Gerber, S. A.; Rudner, A. D.; Beausoleil, S. A.; Haas, W.; Villen, J.; Elias, J. E.; Gygi, S. P. Large-scale phosphorylation analysis of alpha-factor-arrested *Saccharomyces cerevisiae*. *J. Proteome Res.* **2007**, *6* (3), 1190–7.
- (19) Matsuoka, S.; Ballif, B. A.; Smogorzewska, A.; McDonald, E. R., 3rd; Hurov, K. E.; Luo, J.; Bakalarski, C. E.; Zhao, Z.; Solimini, N.; Lerenthal, Y.; Shiloh, Y.; Gygi, S. P.; Elledge, S. J. ATM and ATR substrate analysis reveals extensive protein networks responsive to DNA damage. *Science* **2007**, *316* (5828), 1160–6.
- (20) Olsen, J. V.; Blagoev, B.; Gnad, F.; Macek, B.; Kumar, C.; Mortensen, P.; Mann, M. Global, in vivo, and site-specific phosphorylation dynamics in signaling networks. *Cell* **2006**, *127* (3), 635–48.
- (21) Trinidad, J. C.; Thalhammer, A.; Specht, C. G.; Lynn, A. J.; Baker, P. R.; Schoepfer, R.; Burlingame, A. L. Quantitative analysis of synaptic phosphorylation and protein expression. *Mol. Cell. Proteomics* **2008**, *7* (4), 684–96.
- (22) Nguyen, V.; Cao, L.; Lin, J. T.; Hung, N.; Ritz, A.; Yu, K.; Jianu, R.; Ulin, S. P.; Raphael, B. J.; Laidlaw, D. H.; Brossay, L.; Salomon, A. R. A new approach for quantitative phosphoproteomic dissection of signaling pathways applied to T cell receptor activation. *Mol. Cell. Proteomics* **2009**, *8* (11), 2418–31.
- (23) Zanivan, S.; Gnad, F.; Wickstrom, S. A.; Geiger, T.; Macek, B.; Cox, J.; Fassler, R.; Mann, M. Solid tumor proteome and phosphoproteome analysis by high resolution mass spectrometry. *J. Proteome Res.* **2008**, *7* (12), 5314–26.
- (24) Anderson, N. L. The roles of multiple proteomic platforms in a pipeline for new diagnostics. *Mol. Cell. Proteomics* **2005**, *4* (10), 1441–4.
- (25) Lange, V.; Malmstrom, J. A.; Didion, J.; King, N. L.; Johansson, B. P.; Schafer, J.; Rameseder, J.; Wong, C. H.; Deutsch, E. W.; Brusniak, M. Y.; Buhlmann, P.; Bjorck, L.; Domon, B.; Aebersold, R. Targeted quantitative analysis of *Streptococcus pyogenes* virulence factors by multiple reaction monitoring. *Mol. Cell. Proteomics* **2008**, *7* (8), 1489–500.
- (26) Kuhn, E.; Wu, J.; Karl, J.; Liao, H.; Zolg, W.; Guild, B. Quantification of C-reactive protein in the serum of patients with rheumatoid arthritis using multiple reaction monitoring mass spectrometry and ¹³C-labeled peptide standards. *Proteomics* **2004**, *4* (4), 1175–86.
- (27) Anderson, L.; Hunter, C. L. Quantitative mass spectrometric multiple reaction monitoring assays for major plasma proteins. *Mol. Cell. Proteomics* **2006**, *5* (4), 573–88.
- (28) Keshishian, H.; Addona, T.; Burgess, M.; Kuhn, E.; Carr, S. A. Quantitative, multiplexed assays for low abundance proteins in plasma by targeted mass spectrometry and stable isotope dilution. *Mol. Cell. Proteomics* **2007**, *6* (12), 2212–29.
- (29) Keshishian, H.; Addona, T.; Burgess, M.; Mani, D. R.; Shi, X.; Kuhn, E.; Sabatine, M. S.; Gerszten, R. E.; Carr, S. A. Quantification of cardiovascular biomarkers in patient plasma by targeted mass spectrometry and stable isotope dilution. *Mol. Cell. Proteomics* **2009**, *8* (10), 2339–49.
- (30) van 't Veer, L. J.; Dai, H.; van de Vijver, M. J.; He, Y. D.; Hart, A. A.; Mao, M.; Peterse, H. L.; van der Kooy, K.; Marton, M. J.; Witteveen, A. T.; Schreiber, G. J.; Kerkhoven, R. M.; Roberts, C.; Linsley, P. S.; Bernards, R.; Friend, S. H. Gene expression profiling predicts clinical outcome of breast cancer. *Nature* **2002**, *415* (6871), 530–6.
- (31) Masuda, T.; Tomita, M.; Ishihama, Y. Phase transfer surfactant-aided trypsin digestion for membrane proteome analysis. *J. Proteome Res.* **2008**, *7* (2), 731–40.
- (32) Matsumoto, M.; Oyamada, K.; Takahashi, H.; Sato, T.; Hatakeyama, S.; Nakayama, K. I. Large-scale proteomic analysis of tyrosine-phosphorylation induced by T-cell receptor or B-cell receptor activation reveals new signaling pathways. *Proteomics* **2009**, *9* (13), 3549–63.

- (33) Kokubu, M.; Ishihama, Y.; Sato, T.; Nagasu, T.; Oda, Y. Specificity of immobilized metal affinity-based IMAC/C18 tip enrichment of phosphopeptides for protein phosphorylation analysis. *Anal. Chem.* **2005**, *77* (16), 5144–54.
- (34) Taus, T.; Kocher, T.; Pichler, P.; Paschke, C.; Schmidt, A.; Henrich, C.; Mechtler, K. Universal and confident phosphorylation site localization using phosphoRS. *J. Proteome Res.* **2011**, *10* (12), 5354–62.
- (35) Martins-de-Souza, D.; Guest, P. C.; Vanattou-Saifoudine, N.; Rahmoune, H.; Bahn, S. Phosphoproteomic differences in major depressive disorder postmortem brains indicate effects on synaptic function. *Eur. Arch. Psychiatry Clin. Neurosci.* **2012**.
- (36) Jarvinen, T. A.; Tanner, M.; Barlund, M.; Borg, A.; Isola, J. Characterization of topoisomerase II alpha gene amplification and deletion in breast cancer. *Genes, Chromosomes Cancer* **1999**, *26* (2), 142–50.
- (37) Nielsen, K. V.; Muller, S.; Moller, S.; Schonau, A.; Balslev, E.; Knoop, A. S.; Ejlersen, B. Aberrations of ERBB2 and TOP2A genes in breast cancer. *Mol. Oncol.* **2010**, *4* (2), 161–8.
- (38) Futreal, P. A.; Liu, Q.; Shattuck-Eidens, D.; Cochran, C.; Harshman, K.; Tavtigian, S.; Bennett, L. M.; Haugen-Strano, A.; Swensen, J.; Miki, Y.; et al. BRCA1 mutations in primary breast and ovarian carcinomas. *Science* **1994**, *266* (5182), 120–2.
- (39) O'Donovan, P. J.; Livingston, D. M. BRCA1 and BRCA2: breast/ovarian cancer susceptibility gene products and participants in DNA double-strand break repair. *Carcinogenesis* **2010**, *31* (6), 961–7.
- (40) Castilla, L. H.; Couch, F. J.; Erdos, M. R.; Hoskins, K. F.; Calzone, K.; Garber, J. E.; Boyd, J.; Lubin, M. B.; Deshano, M. L.; Brody, L. C.; et al. Mutations in the BRCA1 gene in families with early-onset breast and ovarian cancer. *Nat. Genet.* **1994**, *8* (4), 387–91.
- (41) Kim, S. J.; Nakayama, S.; Miyoshi, Y.; Taguchi, T.; Tamaki, Y.; Matsushima, T.; Torikoshi, Y.; Tanaka, S.; Yoshida, T.; Ishihara, H.; Noguchi, S. Determination of the specific activity of CDK1 and CDK2 as a novel prognostic indicator for early breast cancer. *Ann. Oncol.* **2008**, *19* (1), 68–72.
- (42) Nasir, A.; Chen, D. T.; Gruidl, M.; Henderson-Jackson, E. B.; Venkataramu, C.; McCarthy, S. M.; McBride, H. L.; Harris, E.; Khakpour, N.; Yeatman, T. J. Novel molecular markers of malignancy in histologically normal and benign breast. *Pathol. Res. Int.* **2011**, *2011*, 489064.
- (43) Zheng, M. Z.; Zheng, L. M.; Zeng, Y. X. SCC-112 gene is involved in tumor progression and promotes the cell proliferation in G2/M phase. *J. Cancer Res. Clin. Oncol.* **2008**, *134* (4), 453–62.
- (44) Rakha, E. A.; Boyce, R. W.; Abd El-Rehim, D.; Kurien, T.; Green, A. R.; Paish, E. C.; Robertson, J. F.; Ellis, I. O. Expression of mucins (MUC1, MUC2, MUC3, MUC4, MUC5AC and MUC6) and their prognostic significance in human breast cancer. *Mod. Pathol.* **2005**, *18* (10), 1295–304.
- (45) Wei, X.; Xu, H.; Kufe, D. MUC1 oncoprotein stabilizes and activates estrogen receptor alpha. *Mol. Cell* **2006**, *21* (2), 295–305.
- (46) Mulligan, A. M.; Pinnaduwa, D.; Bane, A. L.; Bull, S. B.; O'Malley, F. P.; Andrulis, I. L. CK8/18 expression, the basal phenotype, and family history in identifying BRCA1-associated breast cancer in the Ontario site of the breast cancer family registry. *Cancer* **2011**, *117* (7), 1350–9.
- (47) Busch, T.; Milena, E.; Eiseler, T.; Joodi, G.; Temme, C.; Jansen, J.; Wichert, G. V.; Omary, M. B.; Spatz, J.; Seufferlein, T. Keratin 8 phosphorylation regulates keratin reorganization and migration of epithelial tumor cells. *J. Cell Sci.* **2012**, 2148–59.
- (48) Hu, Q.; Guo, C.; Li, Y.; Aronow, B. J.; Zhang, J. LMO7 mediates cell-specific activation of the Rho-myocardin-related transcription factor-serum response factor pathway and plays an important role in breast cancer cell migration. *Mol. Cell Biol.* **2011**, *31* (16), 3223–40.
- (49) Merrell, K. W.; Crofts, J. D.; Smith, R. L.; Sin, J. H.; Kmetzsch, K. E.; Merrell, A.; Miguel, R. O.; Candelaria, N. R.; Lin, C. Y. Differential recruitment of nuclear receptor coregulators in ligand-dependent transcriptional repression by estrogen receptor-alpha. *Oncogene* **2011**, *30* (13), 1608–14.
- (50) Hartmaier, R. J.; Tchatchou, S.; Richter, A. S.; Wang, J.; McGuire, S. E.; Skaar, T. C.; Rae, J. M.; Hemminki, K.; Sutter, C.; Ditsch, N.; Bugert, P.; Weber, B. H.; Niederacher, D.; Arnold, N.; Varon-Mateeva, R.; Wappenschmidt, B.; Schmutzler, R. K.; Meindl, A.; Bartram, C. R.; Burwinkel, B.; Oesterreich, S. Nuclear receptor coregulator SNP discovery and impact on breast cancer risk. *BMC Cancer* **2009**, *9*, 438.
- (51) Lemeer, S.; Heck, A. J. The phosphoproteomics data explosion. *Curr. Opin. Chem. Biol.* **2009**, *13* (4), 414–20.
- (52) Larsen, M. R.; Thingholm, T. E.; Jensen, O. N.; Roepstorff, P.; Jorgensen, T. J. Highly selective enrichment of phosphorylated peptides from peptide mixtures using titanium dioxide microcolumns. *Mol. Cell. Proteomics* **2005**, *4* (7), 873–86.
- (53) Rush, J.; Moritz, A.; Lee, K. A.; Guo, A.; Goss, V. L.; Spek, E. J.; Zhang, H.; Zha, X. M.; Polakiewicz, R. D.; Comb, M. J. Immunoaffinity profiling of tyrosine phosphorylation in cancer cells. *Nat. Biotechnol.* **2005**, *23* (1), 94–101.
- (54) Dephoure, N.; Zhou, C.; Villen, J.; Beausoleil, S. A.; Bakalarski, C. E.; Elledge, S. J.; Gygi, S. P. A quantitative atlas of mitotic phosphorylation. *Proc. Natl. Acad. Sci. U. S. A.* **2008**, *105* (31), 10762–7.
- (55) Ostasiewicz, P.; Zielinska, D. F.; Mann, M.; Wisniewski, J. R. Proteome, phosphoproteome, and N-glycoproteome are quantitatively preserved in formalin-fixed paraffin-embedded tissue and analyzable by high-resolution mass spectrometry. *J. Proteome Res.* **2010**, *9* (7), 3688–700.
- (56) Whiteaker, J. R.; Lin, C.; Kennedy, J.; Hou, L.; Trute, M.; Sokal, I.; Yan, P.; Schoenherr, R. M.; Zhao, L.; Voytovich, U. J.; Kelly-Spratt, K. S.; Krasnoselsky, A.; Gafken, P. R.; Hogan, J. M.; Jones, L. A.; Wang, P.; Amon, L.; Chodosh, L. A.; Nelson, P. S.; McIntosh, M. W.; Kemp, C. J.; Paulovich, A. G. A targeted proteomics-based pipeline for verification of biomarkers in plasma. *Nat. Biotechnol.* **2011**, *29* (7), 625–34.
- (57) Addona, T. A.; Shi, X.; Keshishian, H.; Mani, D. R.; Burgess, M.; Gillette, M. A.; Clauser, K. R.; Shen, D.; Lewis, G. D.; Farrell, L. A.; Fifer, M. A.; Sabatine, M. S.; Gerszten, R. E.; Carr, S. A. A pipeline that integrates the discovery and verification of plasma protein biomarkers reveals candidate markers for cardiovascular disease. *Nat. Biotechnol.* **2011**, *29* (7), 635–43.
- (58) Atrih, A.; Turnock, D.; Sellar, G.; Thompson, A.; Feuerstein, G.; Ferguson, M. A.; Huang, J. T. Stoichiometric quantification of Akt phosphorylation using LC-MS/MS. *J. Proteome Res.* **2010**, *9* (2), 743–51.
- (59) Jin, L. L.; Tong, J.; Prakash, A.; Peterman, S. M.; St-Germain, J. R.; Taylor, P.; Trudel, S.; Moran, M. F. Measurement of protein phosphorylation stoichiometry by selected reaction monitoring mass spectrometry. *J. Proteome Res.* **2010**, *9* (5), 2752–61.
- (60) Tong, J.; Taylor, P.; Peterman, S. M.; Prakash, A.; Moran, M. F. Epidermal growth factor receptor phosphorylation sites Ser991 and Tyr998 are implicated in the regulation of receptor endocytosis and phosphorylations at Ser1039 and Thr1041. *Mol. Cell. Proteomics* **2009**, *8* (9), 2131–44.
- (61) Wolf-Yadlin, A.; Hautaniemi, S.; Lauffenburger, D. A.; White, F. M. Multiple reaction monitoring for robust quantitative proteomic analysis of cellular signaling networks. *Proc. Natl. Acad. Sci. U. S. A.* **2007**, *104* (14), 5860–5.
- (62) Thingholm, T. E.; Bak, S.; Beck-Nielsen, H.; Jensen, O. N.; Gaster, M. Characterization of human myotubes from type 2 diabetic and nondiabetic subjects using complementary quantitative mass spectrometric methods. *Mol. Cell. Proteomics* **2011**, *10* (9), M110 006650.
- (63) Muraoka, S.; Kume, H.; Watanabe, S.; Adachi, J.; Kuwano, M.; Sato, M.; Kawasaki, N.; Kodera, Y.; Ishitobi, M.; Inaji, H.; Miyamoto, Y.; Kato, K.; Tomonaga, T. Strategy for SRM-based verification of biomarker candidates discovered by iTRAQ method in limited breast cancer tissue samples. *J. Proteome Res.* **2012**, *11* (8), 4201–10.

